HIGH DYNAMIC RANGE IMAGE ACQUISITION USING FLASH IMAGE

*Ryo Matsuoka, Tatsuya Baba, Masahiro Okuda**

Univ. of Kitakyushu,
Faculty of Environmental Engineering, JAPAN

Keiichiro Shirai

Shinshu University
Faculty of Engineering, JAPAN

ABSTRACT

We propose a denoising technique using multiple exposure image integration. When acquiring a dark scene, the detail of the dark area is often deteriorated by sensor noise. For a high dynamic range image acquisition, denoising in dark areas is a critical issue, since the dark area is, in general, enhanced by a tone-mapping and the noise is made more visible when displaying it on an output devise. In our method, a flash image is utilized as well as no-flash multiple exposure images to further reduce the noise. Multiple exposure integration is performed in a wavelet domain, where noise removal is achieved by the wavelet-shrinkage for multiple exposures. Our method works well especially for noise in shadows. We show the validity of the proposed algorithm by simulating the method with some actual noisy images.

***Index Terms*—** Image denoising, Wavelet transforms, weight function, HDRI, color-line

1. INTRODUCTION

The human visual system can capture a wide dynamic range of irradiance, while the dynamic range of CCD or CMOS sensors does not cover the perceptional range of real scenes. It is important in many applications to catch a wide range of irradiance of a natural scene and preserve the irradiance value in each pixel. In the application of CG, a high dynamic range image (HDRI) is widely used for high quality rendering with image based lighting [1]. In addition, recently it has been applied to the surveillance camera, the in-vehicle camera and the photographic development with high resolution, and so on.

In general, the HDRI is generated by combining some photographs taken with multiple exposure settings [2]-[5]. To get a high dynamic range, we should have several photographs with short to long exposures. As usual, the dynamic range is defined by the ratio of darkest and brightest pixel intensities of an image, where the darkest point is usually defined as the lowest value in a range that is not dominated by noise. Thus the image denoising is often required to acquire the high dynamic range. Although the process of multiple exposure integration inherently has a property to reduce the noise [6], it is often insufficient and noises appear especially in a dark area. When taking photos with a hand held camera in a dark lighting condition, a high ISO setting is required to restore the dark area without blurring artifacts, which yields noisy images and then brings down the dynamic range.

In the last decade, to improve the noise due to a high ISO setting, many techniques [7]-[8] have been proposed based on a flash image. In these methods [7]-[8], a noise-free flash image is converted into a no-flash image while keeping sharp edges and vivid colors. They focus on the ”color-line” [9], that is, color distributions of a local region become linear or planar. Additionally, they consider distortions of a distribution caused by shadows and specular lights, and transform the color distribution of the flash image into the no-flash image by weighted affine transform correctly.

In this paper, we propose an integration technique of the multiple exposure images. The main contribution of the proposed method includes: (I) restoration of high exposure Image by flash/no-flash integration, and (II) high dynamic range image acquisition in the wavelet domain. Our image restoration method is able to preserve more detail in contrast than the conventional methods and outperforms them in denoising capability.

In following sections, we introduce a technique for combining the multiple exposure images. In the method, the high exposure image is restored by a flash image, then the images are combined in the wavelet domain. By employing a sparse approximation in the wavelet expansion, high performance in denoising is achieved.

2. PROPOSED METHOD

2.1. Outline

Fig. 1 shows the procedure of our restoration algorithm. Our method mainly consists of two steps: (I) Restoration of high exposure Image by using flash image, and (II) image integration in the wavelet domain. Unlike the conventional multiple exposure integration, we use a flash image as well as no-flash multiple exposure images. The flash image is utilized to restore dark (low irradiance) regions in a high exposure image, which is described in Sec.2.2 in detail. In the second step, we integrate the multiple exposure images that includes the restored high exposure image. To integrate the multiple exposures, the images are converted to radiance domain by compensating the nonlinearity of a sensor to linearize the response. A weighting function, which is designed to reduce the error, is multiplied to the images. Then, denoising procedure is applied to them. In our method, two types of the wavelet shrinkage is performed, which is explained in Sec.2.4.

2.2. Restoration of High Exposure Image by Flash Image

When acquiring high dynamic range images, one often suffers from sensor noise that appears especially in a dark scene. Since a dark area is often enhanced by a tone-mapping operator, the noise in the shadows is made more visible. Thus the denoising in shadows is a critical problem. In our framework, the dark area of the scene

*Thanks to JSPS and KDDI foundation for funding.

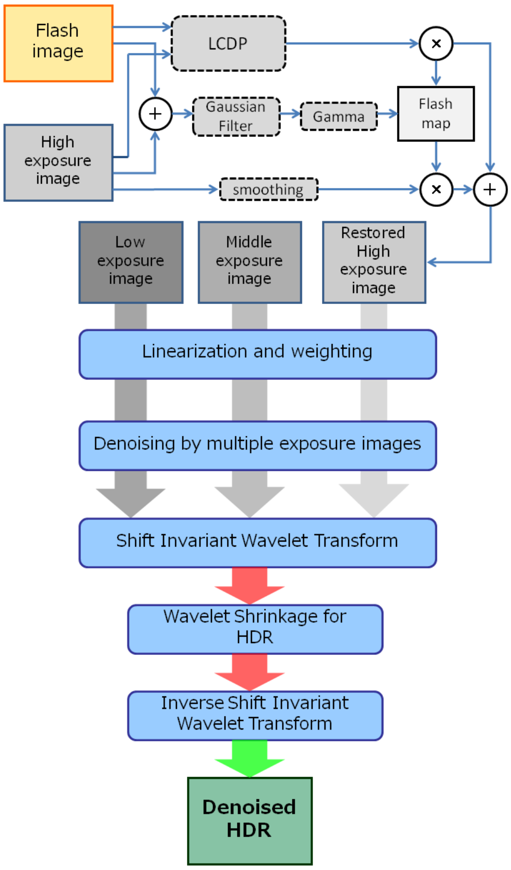

Fig. 1. High exposure image restoration flow.

is mainly restored by the high exposure image. Our aim here is to denoise the high exposure image by using the flash image. The procedure is shown in the upper part of Fig. 1.

For denoising, our method utilizes the property of the local color linearity [8],[9], that is, the RGB distribution of a local window can be approximated as a single line in the RGB space. Figure 2 shows a local region of a flash and no-flash image (a), (b) and their color distributions (c). We can see from the figure that the two color distributions of the no-flash image can be approximated by the affine transform of the flash image. Thus the aim of the restoration here is to find the affine transform that satisfies

$$\boldsymbol{p}_i \approx \boldsymbol{A}_i \boldsymbol{f}_i + \boldsymbol{b}_i,$$

where $\boldsymbol{A}$ and $\boldsymbol{b}$ are 3×3 transform matrix and 3×1 shift vector, $\boldsymbol{f}$ and $\boldsymbol{p}$ are 3×1 RGB vectors of the flash and high exposure (i.e. no-flash) images, respectively. The subscript i is a pixel index.

The RGB color of the flash image is transformed by the matrix $\boldsymbol{A}$. The affine transform $\boldsymbol{A}$ and $\boldsymbol{b}$ are determined by minimizing the cost function:

$$E = \sum_i \sum_{j \in N(i)} \left\{ \omega_{i,j} \cdot \rho\left(\boldsymbol{A}_i \boldsymbol{f}_j + \boldsymbol{b}_i - \boldsymbol{p}_j\right) + \lambda \|\boldsymbol{b}_i\|_2^2 + \epsilon \|\boldsymbol{A}_i\|_F^2 \right\}, \tag{1}$$

where $\omega_{i,j}$ is a bilateral weighting function [8], and ρ is a robust function. We found that the luminance difference between the flash and no-flash images can be compensated by scaling rather than shifting. Therefore, in our case, a large shift vector sometimes adversely affects the results. Thus we added the penalty term $\lambda \|\boldsymbol{b}_i\|^2$ to the cost.

(a)flash, (b) no-flash

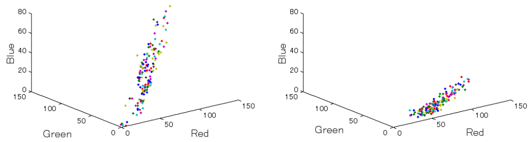

(c) color line of (left) flash, and (right) no-flash

Fig. 2. Linearity of color distributions in corresponding local regions of no-flash and flash images.

If one chooses $\rho(\boldsymbol{x}) = \sqrt{\boldsymbol{x}^t \boldsymbol{x}}$, $\omega_{i,j} = 1$ and $\lambda = 0$, Eq.(1) coincides with the formulation of the guided filter [10]. In our case, we use $p(x) = (-\sigma_s^2/2)\exp(-\|x\|^2/\sigma_s^2)$ to reduce the effect of outliers. In practice, we minimize (1) by using the IRLS (Iterative Reweighted Least Squares) method (for detail, see [8]). Once the optimal transform, which consists of $\hat{\boldsymbol{A}}$ and $\hat{\boldsymbol{b}}$, is found, a restored image is calculated by

$$\hat{\boldsymbol{p}}_i = \frac{C_i}{W_i}, \quad \begin{cases} C_i = \sum_j \omega_{i,j} \hat{\boldsymbol{A}}_j \boldsymbol{f}_j + \hat{\boldsymbol{b}}_j \\ W_i = \sum_j \omega_{i,j} \end{cases} \tag{2}$$

We call this procedure the LCDP (Local Color Distribution Projection).

2.3. Alpha map

For the region where the flash fully reaches, the proposed restoration method in the previous section is used, while we apply the conventional bilateral smoothing [16] for the other region. To discriminate the two regions, we generate an alpha map, which has large values in the region where the flash sufficiently reaches, and has small values in the no-flash regions. Based on the alpha map, we merge the images. The step is described as follows.

We use the flash image $\boldsymbol{f}$ and the high exposure image $\boldsymbol{p}$. To generate the flash map, we estimate the irradiance of the images:

$$R_p = \left(a_p \cdot g^{-1}(\boldsymbol{p})\right)/t_p, \tag{3}$$

where a_p and t_p are the gain of the ISO sensitivity and the shutter speed of $\boldsymbol{p}$. g^{-1} is the camera response curve. R_p is the estimated irradiance. The irradiance of the flash image R_f is also calculated. Then, we find the alpha map Ω:

$$\Omega = M_a\left(R_f - R_p\right), \tag{4}$$

where M_a is a masking function that has 0 in saturated pixels either of the flash or high exposure images. The pixel values of Ω are normalized to the range of [0, 1]. Additionally we apply smoothing filter and gamma correction to Ω in order to make it robust to noises. Based on Ω, we merge the images:

$$p^{'} = \Omega\bar{p} - (1-\Omega)\,\hat{p}. \tag{5}$$

where $\bar{p}$ is the image smoothed by the bilateral filter.

2.4. Denoising by Shrinkage

After the high exposure image is restored, we integrate the multiple exposure images. Before the integration, difference (noise) between the images is relieved in an inter-image shrinkage as follows. First we divide the images to L_m and H_m using (6) and (7).

$$L_m(n) = \frac{M_m(n)p_m\,(n) + M_m(n+1)p_m\,(n+1)}{2}, \tag{6}$$

$$H_m(n) = \frac{M_m(n)p_m\,(n) - M_m(n+1)p_m\,(n+1)}{2}, \tag{7}$$

where $n = 1, \cdots, N-1$, and N is the number of multiple exposures. We assume that lower value of n indicate lower exposure. $p_m\,(n)$ is the $m = \{red, green, blue\}$ channel of the n-th exposure, and $M_m(n)$ is a masking function that has 0 if the original image is 0 (under exposure) or 1 (over exposure), and has 1 otherwise. After the decomposition, we apply hard thresholding to H_m in (7).

$$H_m^*(n) = \begin{cases} 0, & if\ \ H_{m=G}(n) < threshold \\ H_m(n), & otherwise \end{cases}, \tag{8}$$

This determination of thresholding is performed only for the green channel, and if $H_{m=G}(n) < threshold$ at a pixel, the coefficients of the three channels are set to zero, since if the thresholding is performed for the three channels independently, color balance is often destroyed. After the thresholding, we reconstruct the images by

$$p_m^*\,(n) = L_m(n) + H_m^*(n). \tag{9}$$

In the second step, we integrate the images in the wavelet domain. In general, a low exposure yields a dark image and its low pixel values with noises are enhanced by the camera response curve and the tone-mapping operator. Summing up images may remove the noise to some extent [6]. However the simple integration does not always remove noises adequately. In this section we try to remove the noise by shrinkage for multiple exposure image.

Before applying the wavelet transform, we weight the image by

$$p_m'\,(n) = w_m\,(n) \cdot p_m\,(n)\,, \tag{10}$$

where we use the weight function of [18], which is expressed by

$$w(i) = m_f(i) \cdot \frac{1}{(b_1 + b_2 g(i) + b_3 g'(i))/t} \tag{11}$$

where g' is the derivative of g, and $m_f(i)$ is a masking function that has 0 in the saturation pixel. Using this weight function, one can control the suppression effect of the sensor noise and quantization error by varying the parameters. Here $b_1 = 0.001$, $b_2 = 0.01$, $b_3 = 0.001$ are used and fixed for all images. This paper aims at removal of the dark area's noise, and so the weight function by the above parameter setup reduces a sensor noise.

Next, we employ the wavelet shrinkage to our integration problem to remove the noise. The weighted images, p_m' in (10) is converted by the Haar-based shift invariant wavelet transform (non-subsampling). In the wavelet conversion, a low pass/high pass filter pair is performed to it in the horizontal and vertical direction respectively, and four subbands (LL, HL, LH, and HH) are produced, and then repeatedly the LL band is transformed to four bands.

Here we introduce the wavelet shrinkage for the multiple exposure integration. We modify the shrinkage [11], [12] to a multiple exposure integration. The problem is defined to minimize the cost function:

$$\min_h E(h) = |h|^0 + \lambda \sum_{n=1}^{N} (h - h(n))^2, \tag{12}$$

where $h\,(n)$ is an input wavelet coefficient of the weighted n-th exposure image and h is an output wavelet coefficient formed by the high dynamic range. Additionally, λ is the parameter to control noise removal. By differentiating $E(h)$ with respect to h and setting it to 0, we derive the optimal wavelet coefficients:

$$h^* = \begin{cases} 0, & if\ \ 1 - \lambda\left(\frac{1}{N}\sum_n h(n)\right)^2 > 0 \\ \frac{1}{N}\sum_n h(n), & otherwise \end{cases}. \tag{13}$$

The lowest band is simply merged by the weighted mean. Note that roles of (13) are not only the shrinkage based denoising but also multiple exposure fusion in the wavelet domain in which it is different from the conventional shrinkage.

3. EXPERIMENTAL RESULTS

To evaluate the method quantitatively, we artificially created ground truth as follows. First we prepare three images with different exposures, each of which is obtained by averaging 15 photographs, and we select randomly one of them for each as input images. Then the three images are integrated by conventional method and our method. In our method, we have a flash image as an input as well.

First we compare the results of high exposure image restoration described in Sec.2.2 to confirm the validity of the LCDP. Fig.3 shows four images of high exposure image: the ground truth, noisy image, our result, and the result of the conventional method [7]. Our method and [7] use the flash image as a second input. One can see from the figure that denoising capability of the two methods are almost same, but our method preserves more detail than [7].

Next we show the results of the multiple exposure integration. The results of our method, the conventional integration (simple weighted sum of the images), BM3D [15] and Bilateral filter [16] are shown in Fig.4. The image at the top is the tone-mapped version of a ground truth HDR image. Table 1 indicates the quantitative results (PSNR) of three images (a)-(c). We enhance the detail of the images by the three methods: Reinhard's method [1], Jinno et al.'s method [17], and tone-map function (tonemap.m) in MATLAB image processing toolbox, and calculate the PSNR of the tone-mapped images. The results show that our method outperforms the others.

4. CONCLUSION

We proposed a method for the HDR acquisition with detail restoration, especially the extremely dark scene. The proposed method can significantly restore the detail of dark area compared with the conventional integration method and some denoising technique.

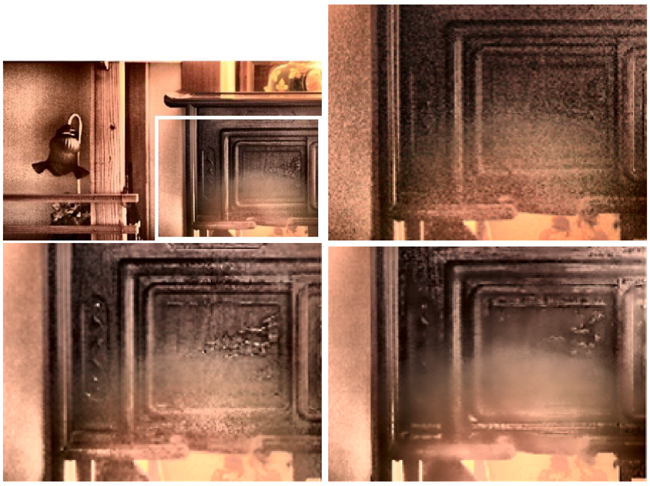

PSNR 38.93, PSNR 38.16

Fig. 3. Result: (upper left) Full frame of ground truth, (upper right) Input, (lower left) Our method, (lower right) Petschnigg et al. [7]

Table 1. Comparison in PSNR for images (a)-(c)

Tone-mapping		**[1]**	**[17]**	**MAT**
conventional method	(a)	28.31	21.24	22.30
	(b)	27.87	20.21	22.37
	(c)	30.17	19.56	23.38
our method	(a)	30.14	24.34	27.97
	(b)	29.93	24.02	25.70
	(c)	32.15	22.62	23.60
BM3D	(a)	28.46	21.81	22.33
	(b)	27.96	20.80	22.08
	(c)	28.23	17.71	23.54
Bilateral Filter	(a)	28.21	21.70	22.38
	(b)	27.34	19.94	22.01
	(c)	27.78	17.87	23.22

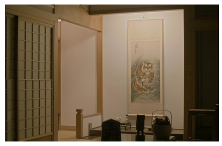

(a) Image 1

(b) Image 2

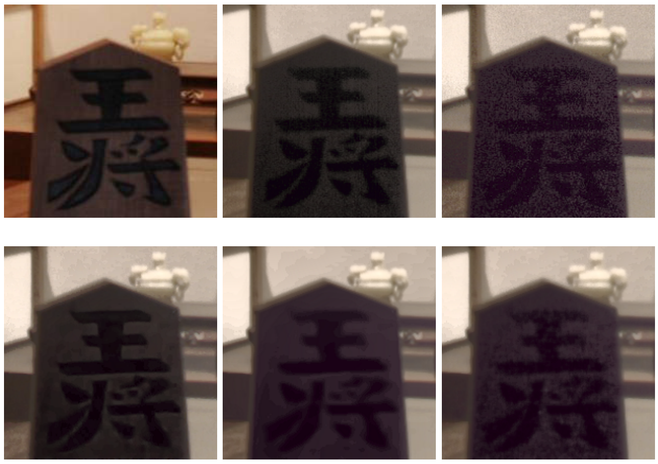

(c) Results of Image 1

(d) Results of Image 2

Fig. 4. Result: (top left) Flash image, (top middle) Ground truth, (top right) Noisy image, (lower left) our method, (lower middle) BM3D, (lower right) BRF

5. REFERENCES

[1] E. Reinhard, S.Pattanaik, G. Ward and P. Debevec, ”High Dynamic Range Imaging: Acquisition, Display, and Image-Based Lighting (Morgan Kaufmann Series in Computer Graphics and Geometric Modeling),” *Morgan Kaufmann Publisher 2005*.

[2] P.E. Debevec and J. Malik.”Recovering High Dynamic Range Radiance Maps from Photographs,” Proceedings of SIGGRAPH 97, Computer Graphics Proceedings, pp. 369-378 . 1997

[3] S. Mann and R. Picard, ”On being ’undigital’ with digital cameras: Extending dynamic range by combining differently exposed pictures,” In Proceedings of IS&T 46th annual conference (May 1995), pp. 422–428. 1995

[4] T. Mitsunaga, and S. K. Nayer,”Radiometric Self Calibration,” IEEE Conference on Computer Vision and Pattern Recognition (CVPR), Vol.1, pp.374-380, Jun, 1999.

[5] T. Jinno, and M. Okuda, ”Motion blur free HDR image acquisition using multiple exposures,” IEEE International Conference on Image Processing, pp. 1304 - 1307, Oct. 2008

[6] T.Buades, Y. Lou, J.M. Morel and Z. Tang, ”A note on multi-image denoising,” International workshop on Local and Non-local Approximation in Image Processing, pp.1-15, Aug. 2009.

[7] G. Petschnigg, R. Szeliski, M. Agrawala, M. Dohen, H. Hoppe, and K. Toyama, ”Digital photography with flash and no-flash image paris,” in ACM Trans. on Graphics (SIGGRAPH), vol. 23, pp. 664-672, 2004

[8] K. Shirai, M. Ikehara, M. Okamoto, ”Noiseless no-flash photo creation by color transform of flash image, ” Inter. Conf. on Image Proc. (ICIP), 2011 Sep.

[9] L. Orner and R. Werman, ”Color lines: Image specific color representation,” in IEEE Conf. on Computer Vision and Pattern Recognition, 2004, vol. 2, pp. 946-953.

[10] Kaiming He, Jian Sun, and Xiaoou Tang. ”Guided image filtering”, In Proceedings of the 11th European conference on Computer vision: Part I (ECCV’10), pp.1-14, 2010.

[11] R.H. Chan, R.F. Chan, L. Shen, and Z. Shen, ”Wavelet algorithms for high-resolution image reconstruction,” SIAM J. Sci. Comput. 24, pp. 1408-1432, 2002.

[12] T. Saito, N. Fujii, and T. Komatsu, ”Iterative soft color-shrinkage for color-image denoising,” IEEE International Conference on Image Processing, pp.3837-3840, Nov. 2009

[13] Zuiderveld, Karel. ”Contrast Limited Adaptive Histograph Equalization.” Graphic Gems IV. San Diego: Academic Press Professional, pp.474-485. 1994.

[14] Zhou Wang, Alan C. Bovik, Hamid R. Sheikh, and Eero P. Simoncelli, “ Image quality assessment: From error visibility to structural similarity, ” IEEE Trans. Image Process., vol. 13, no.4, pp.600-612, 2004.

[15] K. Dabov, A. Foi, and K. Egiazarian, “ Image restoration by sparse 3D transform-domain collaborative filtering, ” Proc. SPIE Electronic Imaging ’08, no. 6812-07, San Jose, California, USA, January 2008.

[16] C. Tomasi and R. Manduchi, ”Bilateral filtering for gray and color images,” in Proc. IEEE Inter Conf. on Computer Vision, 1998, pp. 839-846.

[17] Takao Jinno, Hiroya Watanabe, Masahiro Okuda, ”High Contrast Tone-mapping and its Application for Two-layer High Dynamic Range Coding”, APSIPA Annual Summit & Conference, Dec. 2012 (to appear)

[18] Ryo Matsuoka, Masahiro Okuda, ”Multiple Exposure Integration with Image Denoising”, APSIPA Annual Summit & Conference, Dec. 2012 (to appear)